A THEORETICAL INVESTIGATION OF THE EFFECT OF UPWASH AND CAMBER ON DRAG DUE TO LIFT FOR RECTANGULAR WINGS AT SUPERSONIC SPEEDS

Thesis by

Oscar Seidman

In Partial Fulfillment of the Requirements

for the Degree of

Aeronautical Engineer

California Institute of Technology

Pasadena, California

1955

ACKNOWLEDGEMENT

The author desires to express his appreciation to Professor Paco Lagerstrom who suggested the study of this problem and under whose guidance the investigation was carried out.

ABSTRACT

A theoretical investigation was conducted, using linearized theory, to determine the combined effects of upwash and camber on drag due to lift for rectangular wings at supersonic speeds. Both the case of body upwash and the case of a uniform upwash field were considered. Previous studies have shown that body upwash and wing camber, acting separately, each reduce the drag due to lift for a rectangular wing. In the present investigation it was found that the individual effects as measured by the criterion $\ell = \frac{C_L^2}{C_D}$ are additive and that there is a further gain which increased with decreasing aspect ratio. For the basic wing-body configuration investigated, with wing having a reduced aspect ratio of two, the upwash effect was much larger than the camber effect. For a complete aircraft configuration with lifting nose, optimum camber reduced the drag at a given lift by a somewhat smaller percentage than it did for an isolated wing. The analysis further indicated that use of moderate negative wing incidence could reduce aircraft drag at a given lift.

TABLE OF CONTENTS

LIST OF TABLES

LIST OF FIGURES

I. INTRODUCTION

Supersonic aircraft experience viscous drag, thickness drag, and drag due to lift. In the linearized theory of non-viscous flow it is permissible to represent any wing as the sum of a symmetric wing (thickness distribution) plus a lifting wing of zero thickness, and to consider their effects separately. The current theoretical study deals with lift and the associated drag of the latter type of wing.

Previous investigations have covered the independent effects of upwash and camber on drag due to lift for rectangular wings. Reference 1 presented a simplified method for determining the lift of a flat rectangular wing as influenced by the upwash field from a cylindrical fuselage. In reference 2 this method was applied in estimating the drag reduction at a given lift, attributable to this upwash. In references 3 and 4 it was brought out that for an isolated rectangular wing in a free-stream flow (no upwash) appropriate camber will reduce the drag at a given lift.

The present investigation is concerned with the combined effects of upwash and camber on drag due to lift for rectangular wings. The wing planform is fixed while assessing the effects of camber and upwash, but the influence of aspect ratio is also determined independently. Two general configurations are analyzed. In one case the wing is mounted at zero incidence on the diameter of a circular fuselage which is "long" forward of the wing and terminates at the wing trailing edge. In the other case an isolated tail surface is located in a uniform upwash field. The camber is

assumed to be symmetric about the midchord and is constant across the span. Camber lines composed of flat segments or having continuous curvature were considered. The effects of body nose lift and of wing incidence are examined qualitatively. Body "nose" refers herein to the portion of the body forward of the wing leading edge.

SYMBOLS

a	body radius
A	mean geometric angle of attack of wing
(AR)	aspect ratio of exposed wing (the wing formed by joining the left and right wing roots)
b	span of exposed wing
B	incremental angle of camber for a wing segment (B = kA)
c	chord of wing
C	upwash angle
C_L	lift coefficient, $\frac{L}{qS}$
C_D	drag coefficient, $\frac{D}{qS}$
d	parameter $\frac{C_D}{C_L^2}$ or $\frac{DqS}{L^2}$
D	drag
f	proportionality factor
ℓ	parameter $\frac{C_L^2}{C_D}$ or $\frac{L^2}{DqS}$
k	proportionality factor
L	lift

M	Mach number
n	ratio of installed wing span to body diameter, s/a
N	normal force
P	pressure
q	dynamic pressure
s	semi-span of wing-body combination
S	exposed wing area
u	upwash velocity
V	free-stream velocity
x	chordwise coordinate
y	spanwise coordinate
α	angle of attack
β	cotangent of Mach angle ($\beta = \sqrt{M^2-1}$)
β(AR)	"reduced" aspect ratio

Subscripts:

b	body
g	geometric
R	resultant
u	upwash

II. PHYSICAL CONCEPTS

A. Effect of Upwash

The effect of upwash in reducing the drag due to lift is apparent in figure 1. Figure 1(a) shows a flat-plate rectangular wing at an angle of attack, α_1, with the resultant force normal to the chord. The lift is approximately equal to the normal force and the drag is $L_1 \alpha_1$. In figure 1(b) the lift was doubled by tilting the wing, which gave four times the original drag. In figure 1(c) the lift was doubled by adding a uniform upwash velocity, which gave only twice the original drag. Thus upwash decreases the drag for a given lift.

It was pointed out in reference 5 that for a wing mounted on the diameter of a long circular fuselage, the upwash angle within the body Mach cone is $\alpha_b \frac{a^2}{y^2}$ where α_b is the body angle of attack, a the body radius and y the spanwise distance from the center of the body. This flow field also corresponds to two-dimensional incompressible flow about the body with velocity, $V\alpha_b$, which is the component of free-stream velocity normal to the body axis. The wing is located in a region with normal velocity $V\alpha_b(1 + \frac{a^2}{y^2})$ so that its local angle of attack is $\alpha_b(1 + \frac{a^2}{y^2})$. At the wing root $(\frac{a}{y} = 1)$ the effective wing angle of attack is doubled by the upwash, but the increment decreases rapidly toward the tips. The velocity field is sketched in figure 2. The simplified analysis of reference 1 indicated that when the reduced aspect ratio of the exposed wing is not less than 2, the lift of the wing and intervening body section may be determined by assuming that the two halves of the exposed wing are joined and that the body acts like a vertical plate in preserving the wing lift.

B. Effect of Camber

A simple demonstration of the favorable effect of camber in the wing tip region is given in figure 3. The illustrative example shows that when a small amount of camber is applied by tilting down the forward and rear halves of a flat wing, maintaining constant lift, the loss in drag for the front half wing exceeds the gain in drag for the rear half wing. The same type of analysis can be used to show that a large amount of camber has an adverse effect on drag. The analysis in reference 4, furthermore, shows that when parabolic camber is applied to a rectangular wing at a given angle of attack the gain in lift depends on the first power of the camber while the drag increment increases as the square. Accordingly, a small amount of camber is favorable but an optimum is reached beyond which additional camber is detrimental.

C. Anticipated Effects of Combined Upwash and Camber

From qualitative considerations it seems plausible that the benefits of combined upwash and camber should exceed the sum of their separate effects. When upwash is applied to a cambered wing, more load is added to the forward half of the wing than to the rear half, because of tip losses. Adding most of the load on the part of the wing that is at the lowest geometric angle should be beneficial. Moreover, the optimum camber would tend to be greater when the local angle of attack is increased by the upwash. The separate effects of camber and upwash each tend to become greater at lower aspect ratios, so their combined effects would increase as aspect ratio decreases.

IV. METHOD OF ANALYSIS

A. Criterion of Effectiveness

For a given wing planform and body diameter it is desired to obtain the least drag for a given lift or the most lift for a given drag. The variables that can be controlled are the wing incidence angle, which influences body upwash at a given lift, and the wing camber. The inadequacy of using the lift-to-drag ratio as a criterion is apparent from the fact that for a flat wing this ratio approaches infinity as the lift approaches zero. It would, accordingly, be necessary to specify the lift at which the drag is to be determined. Another criterion, $\ell = \frac{C_L^2}{C_D} = \frac{L^2}{DqS}$, proves to be convenient for most of the analysis made subsequently. ℓ is a measure of $(\text{lift})^2$ for a given drag, while its reciprocal, d, measures drag for a given lift. For a flat wing in a free stream $\ell = \frac{dC_L}{d\alpha}$, which is invariant with α. Its reciprocal measures the drag penalty associated with unit lift. For a cambered wing in a free stream ℓ is invariant with mean geometric angle of attack, provided the camber increases in proportion to this angle. This invariance is discussed in reference 6 and explained briefly in Appendix A. Because of this invariance the optimum ℓ may be determined without the necessity of specifying a definite value of lift. It should be noted that the camber for optimum ℓ is proportional to angle of attack so that a wing which is optimum at one design angle will have to be warped if it is to be made optimum at another angle. For the case of a wing mounted on a circular body at zero incidence, the upwash velocity increases in

proportion to the wing geometric angle of attack. For this case also it can be shown (Appendix A) that the parameter ℓ is invariant with α, provided that the camber is proportional to α. Results obtained through the use of the parameter ℓ can, of course, also be obtained by solving for drag at a given lift. The latter procedure is used herein when comparison is to be made among configurations having different lifting-surface areas.

B. Superposition Procedure to Evaluate Optimum Camber

The basic problem was to evaluate lift and drag for a wing mounted at zero incidence on the rear end of a long cylindrical body. (Body nose forces were disregarded initially.) To simplify the analysis, camber was represented by two flat segments. Figure 4 shows the manner in which the wing-body lift problem is broken down into simpler problems. In figure 4(a) it is seen that the complete configuration may be represented as a superposition of three configurations: a body at angle of attack, a wing with the geometric angle of attack mounted on a body that is at zero angle of attack, and a wing with the upwash-induced angle of attack mounted on a body that is at zero angle of attack. The lift on the body alone is neglected for the present and, as mentioned previously, the lift on each of the two wing-body configurations may be evaluated by analyzing the equivalent wings formed by joining the two halves of the exposed wings. The equivalent geometric wing and the upwash wing are shown in figure 4(a), (6) and (7). Figure 4(b) shows how the equivalent geometric wing may be regarded as a superposition of a flat wing at the mean geometric

angle of attack and a camber-increment wing. The latter wing may be further broken down as shown in figure 4(b)(6). The total wing-body lift was obtained by adding the lifts on the component equivalent wings. This lift was assumed to be acting on the geometric or physical wing. Finally, the drag was determined by taking the product of the lift on each segment of the physical wing by the corresponding angle of attack. Approximations involved in using this method are discussed in a later section. For the case of a flat rectangular wing attached to a circular body of infinite length an expression for the total lift as influenced by upwash was available in reference 2, based on an analysis in reference 7. In order to determine the lift on the front and rear halves of the wing, the solution was obtained in turn for the entire wing and for just the forward half. Because of limitations noted in reference 1, this method was not applied for reduced aspect ratios less than 2. To determine optimum camber and corresponding value of ℓ, the lift and drag were expressed in terms of an unknown amount of camber. An expression for ℓ was then formed and the optimum camber derived as that which makes ℓ a maximum. Other special problems were examined by similar techniques, described subsequently.

V. RESULTS AND DISCUSSION

A. Wing-body Combinations with Zero Wing Incidence

Wing of reduced aspect ratio 2 on standard body.

This is the basic case illustrated in figure 4, which is drawn for a Mach number of $\sqrt{2}$. The span of the installed wing (including its extension through the body) is three times the body diameter. The span of the exposed wing is twice the body diameter and its reduced aspect ratio, $\beta(AR)$, is 2. Unless otherwise indicated, the term "aspect ratio" will be used hereinafter to denote "reduced aspect ratio". The lift to be determined corresponds to what would be measured by taking the pressure distribution over the wing and intervening body. The details of the solution for this case are shown in Appendix B, and the results are summarized in Table 1.

It is seen that the parameter, ℓ, representing $(\text{lift})^2$ for a given drag shows a large gain due to upwash (38.5%), a small gain due to camber (2.1%), and due to combined camber plus upwash the two separate gains are additive and there is a "supplementary gain" amounting to 0.5%. Optimum camber with upwash is larger than without but small variations in camber do not appreciably affect the results. In terms of the reciprocal parameter, d, the percentage decrease in d is smaller than the corresponding gain in ℓ. Moreover, although the separate effects of camber and upwash on d are approximately additive, there is a small supplementary loss in effectiveness when camber and upwash are applied concurrently. It is to be expected, however, that in cases where the supplementary gain in ℓ is very large the magnitude

of the combined effects on d would exceed the sum of the separate effects.

Variations from basic case.

The effects of the principal design variables were investigated by considering other configurations, figure 5, and the results are summarized in Table 2. As would be expected, increasing the aspect ratio by increasing the span decreased the effects of camber and upwash on ℓ and also decreased the supplementary gain. On the other hand, doubling the body diameter to increase the upwash effect increased the supplementary gain from 0.5% for the original body to 0.9% for the larger body. Increasing the number of camber segments from two to three increased the camber effect from 2.1% to 2.5%, and the use of continuous parabolic camber gave a further increase to 2.8%.

The supplementary gain was increased slightly for continuous camber. The method of analysis for continuous camber differed somewhat from the procedure already discussed and is therefore explained in Appendix C. It is interesting to note that the effects for two-segment camber gave a fairly good indication of the effects for continuous camber.

B. Isolated Tail Surfaces in Upwash Field

As upwash and camber effects tended to increase for smaller aspect ratios the investigation was extended to include the aspect ratio of 1. To simplify the analysis the upwash field was assumed to be constant over the lifting surface, corresponding to the case of an isolated tail surface. The superposition

procedure for determining lift on the forward and rear portions of a tail having two-segment camber is illustrated in figure 6. Optimum camber was determined for several values of upwash and the results are summarized in Table 3. For aspect ratio of 1 optimum camber is large, ℓ is small, and the gain in ℓ due to camber amounts to 12.5%. The corresponding decrease in d (or reduction in drag for a given lift) is 11.1%. In an upwash field that increases the mean angle of attack by 20% there is a gain in ℓ of 20% due to the upwash. The independent gains of upwash and camber are additive and there is a supplementary gain of 2.6% of the basic flat-wing-alone value. Doubling the upwash increased the supplementary gain to 5.6%. In terms of the reciprocal parameter, d, camber and upwash each give substantial reductions in drag at a given lift, but their combined effect is somewhat less than the sum of the separate effects. It should be noted, however, that this loss in combined effect is less than what would obtain if there were no supplementary gain in ℓ. So corresponding to the supplementary gain for ℓ there is a decrease in supplementary loss for d.

C. Effects of Wing Incidence and Body Nose Forces

The analysis thus far has been concerned with forces on the wing-body combination without consideration of the additional forces that act on the nose section. Such forces become increasingly important if negative wing incidence is contemplated as a possible means of increasing the favorable effects of body upwash.

The nose lift, unlike wing lift, is not well represented by the linearized theory or even by slender-body theory. This disagreement, as pointed out in reference 8, is caused by the effect of viscous cross flow, which in turn is strongly influenced by Reynolds number. Accordingly, the following extension of the preceding study to include the influence of nose forces, involves arbitrary assumptions and is intended to be interpreted in a qualitative sense.

Body nose forces for zero incidence case.

The body upwash field which was used to improve the wing efficiency in the previous analysis is associated with a lift on the nose section. Slender-body theory, for example page 239 of reference 9, gives for the nose forces due to angle of attack in non-viscous flow: $L = \frac{\pi}{2} q(2a)^2 \alpha$, where 2a is the body diameter, and $D = L\frac{\alpha}{2}$. According to reference 8, this potential flow theory value should be combined with a viscous flow correction giving the form:

$$C_L = k_1\alpha + k_2\alpha^2$$

$$C_D = \tfrac{1}{2}k_1\alpha^2 + k_2\alpha^3$$

where k_2 depends on the viscous drag coefficient of the crossflow. Thus at low α, C_L/C_D approaches $2/\alpha$ and at high α it approaches $\frac{1}{\alpha}$. For the subsequent analysis the slender-body-theory value of body nose lift, $L = \frac{\pi}{2} q(2a)^2\alpha$, is arbitrarily assumed, and is used with the conservative drag relationship, $D = L\alpha$.

The inclusion of nose lift implies a change in lifting area from that of the simpler wing-body problem previously treated.

Accordingly, in lieu of using the parameter ℓ, comparison is made of the values of drag for a given lift. The standard of comparison is the flat wing of aspect ratio 2, at angle of attack A. The effects of the nose forces for the zero-wing-incidence case are shown in Table 4. Inasmuch as the nose lift is independent of β while the wing-body lift depends on β, a specific value, $\beta = 1$, is assumed in obtaining a numerical value for the overall lift. It is seen from Table 4 that inclusion of the nose forces in the upwash problem reduces the drag at a given lift by about 11% of its value for the flat wing alone, or by about 16% of the smaller drag that obtains in the presence of upwash. Evidently this drag reduction occurs because the wing operates at a substantially lower angle of attack when part of the required lift is carried by the nose. The application of camber to the flat wing, including the effects of body upwash and nose forces, reduced the drag at a given lift by 1.5%. This is somewhat smaller than the effect obtained disregarding nose lift because the camber now influences only part of the lifting surface. The magnitude of the total drag reduction attributable to camber, upwash, and nose lift is 40.2%.

Optimum incidence case.

If the wing is installed at negative incidence, then for a given wing geometric angle of attack the body will be at a higher angle, with greater upwash angles and nose forces. It may be anticipated that for small incidence angles the favorable upwash effect would predominate, but that for large angles the adverse effect of body drag would become serious. To explore incidence

effects, computations were made of the drag for a given lift using the wing-body combination of the previous paragraph, but eliminating camber and installing the wing at various negative incidence angles. The nose lift and drag were determined as in the zero-incidence case, and the wing-body lift and drag were determined for $\beta = 1$ as in Appendix B, using equation B9 in lieu of B1. It was found that the least drag for a given lift occurred when the body angle of attack was about four times the wing angle (Fig. 7(a). (Just as the optimum camber varied with wing angle, requiring wing warping, so also the optimum incidence varies with wing angle, requiring a variable-incidence wing.) This incidence gave a drag reduction to 86% of the zero-incidence value. With optimum incidence the optimum amount of two-segment camber was determined as in Appendix B. Application of this camber further reduced the overall drag by 1.4%. These results are included in Table 5, which also summarizes the drag reduction due to camber for the principal configurations with aspect ratio of 2. The drag reduction when a flat wing is replaced by a cambered wing ranges from 2% for an isolated wing to 1.4 or 1.5% for a wing on a body with nose lift. The summary in Table 5 is also significant in bringing out incidence effects. If the zero upwash case is interpreted to represent positive wing incidence such that the body is at zero angle of attack and there are no body forces due to angle of attack, then the drag at a given lift decreases markedly in going from positive to zero incidence and beyond that to negative incidence. Accordingly, from the viewpoint of reduction of

drag due to lift, there seems to be little justification for going to positive wing incidence.

D. General Effect of Camber with Upwash

In the previous sections the effects of combined upwash and camber for the wing-body problem were ordinarily expressed as a percentage of the basic value of the parameters for the flat wing alone, in order to bring out the extent to which the separate effects were additive. The prevalence of the supplementary gain in suggested that a simpler description of the results might be found if the percent change in ℓ were expressed in terms of the initial value of ℓ (i.e. with or without upwash) for which the camber is applied. This has been done in Table 6 and it is seen that a simple and consistent picture of camber effect is obtained. Two-segment camber for the wing of aspect ratio 2 gave the same proportional increase in ℓ, approximately 2 percent, for three different upwash conditions, zero, standard body, and large body. Three-segment camber gave about 2.4 percent and parabolic camber about 2.7 percent for two upwash conditions. Similarly the cambered wing of aspect ratio 1 gave about 12.7 percent increase in ℓ for three widely different upwash values. The effects of camber on d (i.e. the drag reduction due to camber) showed the same consistent trends but tended to run slightly smaller than the corresponding percentages of ℓ. For the range of conditions investigated it may accordingly be generalized that camber gives about the same percentage change in ℓ or d with upwash as without upwash. As the initial value of ℓ is higher with upwash,

this gives a larger actual gain. Similarly, as the initial value of d is smaller with upwash, this gives a numerically smaller decrease in drag at a given lift.

E. Accuracy of the Method

Experimental data pertaining to upwash effects on cambered rectangular wings are apparently not available for comparison with the present theoretical results. Two possible weak spots in the method of analysis used are the arbitrary assumptions used in estimating nose forces and the assumption that the wing-body lift can be represented by the exposed-wing lift.

Because of the large possible variation in nose-force coefficients, the analysis presented herein should be interpreted qualitatively. Where specific information on the force coefficients is available the method illustrated herein may be applied with greater assurance.

With regard to the distribution of pressure between the wing root and the body, some related information is available in reference 10. Pressures were measured (and compared with theoretical predictions) for configurations representing a flat wing at zero incidence on a circular body and a flat wing at negative incidence on a body at zero angle of attack. A trend brought out by the results is that within the flow regions influenced by the wing-body juncture there is a partial transfer of loading from the wing to the body. In a qualitative sense therefore, the previous assumption that the exposed wing carries the entire load requires a correction to allow for appreciable leakage of lift from the rear part

of the wing to the adjacent body. If the rear segment of the cambered wing is at the same geometric angle as the body there will be no change in computed drag. For a cambered wing at zero incidence the body is at a lower angle of attack than the rear wing segment, so leakage of lift would tend to make the combined camber-upwash effect more favorable than previously estimated. For large negative incidence the reverse would be true. For a small negative incidence (approaching optimum incidence), the rear wing segment and body would be at the same angle (fig. 7(b)) so the previous analysis would need no correction. It appears, therefore, that for conventional wing incidences, that is within the range from small negative to large positive values, the estimated beneficial effects of camber presented herein are on the conservative side.

VI. CONCLUDING REMARKS

Effects of combined camber and upwash. Considering the forces on a wing and adjoining section of a circular body the independent beneficial effects of camber and upwash, as measured by the parameter $\ell = \frac{C_L^2}{C_D}$, were additive and there was a supplementary gain which increased as aspect ratio decreased. In terms of the reciprocal parameter, d, the separate effects were approximately additive but there was a small supplementary loss in combined effectiveness for the range of conditions investigated. These results may also be expressed by the statement that camber gave about the same percentage change in ℓ and d for a wing with upwash as it did for a wing in a free stream. For a complete aircraft configuration with a lifting nose, the application of optimum camber reduced the drag at a given lift by a somewhat smaller percentage than it did for an isolated wing.

Effects of off-design operation. As optimum camber is proportional to the wing angle of attack the wing would have to warp or change actual camber to be optimum over a range of angles of attack. It appears, however, that a rigid wing, having optimum camber at one angle of attack, may be used over a wide angle-of-attack range without appreciable loss of effectiveness. As an example, for a wing of aspect ratio 2, optimum continuous camber will increase ℓ by 2.8% at the design angle of attack. If the angle of attack of this rigid cambered wing is doubled or halved, ℓ will still be about 2% greater than for a flat wing.

Reference 11 discusses the compromises that must be made as regards drag due to lift in selecting a rigid aircraft design to give optimum performance for a given mission.

Wing incidence angle. Insofar as concerns attainment of low drag due to lift, the present analysis indicates that positive wing incidence tends to be unfavorable and that moderate negative wing incidence is favorable. Other considerations may, however, be more important in selection of incidence angle.

APPENDIX A

INVARIANCE OF THE PARAMETER ℓ

Wing-alone case

Consider a rectangular wing with arbitrary angle of attack distribution $\alpha_1(x, y)$, as in figure 8(a). Figure 8(b) gives a specific example, with two-segment camber. Assume that when the mean angle of attack is increased by a factor, f, the local angles are similarly increased. This type of wing (which warps with change in angle of attack) is shown in figures 8(c) and 8(d).

The angle of attack distribution, α_2, is proportional to some initial distribution, i. e.

$$\alpha_2(x, y) = f\alpha_1(x, y) \tag{A1}$$

As local pressure is proportional to local angle of attack, it follows that:

$$P_2(x, y) = fP_1(x, y) \tag{A2}$$

Then lift, $$L_2 = \int P_2 dS = f\int P_1 dS \tag{A3}$$

and drag, $$D_2 = \int P_2\alpha_2 dS = f^2\int P_1\alpha_1 dS \tag{A4}$$

Therefore $$\frac{L_2^2}{D_2} = \frac{\left[\int P_1 dS\right]^2}{\int P_1\alpha_1 dS} = \frac{L_1^2}{D_1} \tag{A5}$$

So $\frac{L^2}{D}$ is invariant with α, when local angles are proportional to α.

Wing-body case

If the upwash at any point on the wing increases in proportion to the mean geometric wing angle of attack the pressure increment due to upwash may be written $fk_u(x, y)$.

Then

$$\text{Lift,} \qquad L_2 = f\int (P_1 + k_u)dS \tag{A6}$$

$$\text{Drag,} \qquad D_2 = f^2\int a_1(P_1 + k_u)dS \tag{A7}$$

and again

$\frac{L^2}{D}$ is invariant with α

For constant qS, $\frac{L^2}{DqS} = \ell$ is invariant.

APPENDIX B

CAMBER-UPWASH ANALYSIS FOR $\beta(AR) = 2$, TWO-SEGMENT CAMBER, STANDARD BODY

This case is illustrated in figure 4. The configuration parameters are:

chord, $c = 1$

body radius, $a = 0.5$

span-diameter ratio, $n = s/a = 3$

exposed wing area, $S = 2$

cotangent of Mach angle, $\beta = 1$

reduced aspect ratio of exposed wing $\beta(AR) = 2$

wing incidence = 0

wing mean geometric angle of attack = A

camber increment angle, $B = kA$

The lift on the wing and adjacent body is obtained from the equivalent exposed wings, (5) and (6) of figure 4(b). The body effect is represented by the equivalent wing with angle of attack α_u. To determine the lift on the forward and rear segments of each component wing, the following procedure is used. For wing (5) of figure 4(b), which combines the upwash wing with the mean-geometric-angle wing a solution for total lift, from reference (2), is:

$$\frac{\beta L}{qS} = 4A\left[1 - \frac{1}{2\beta(AR)} + \frac{1}{n-1}\left\{1 - \frac{\beta(AR)}{n-1}\left(1 - \sqrt{1 - \frac{2(n-1)}{n\beta(AR)}}\right)\right\}\right] \qquad (B1)$$

where the term $4A\left[1 - \frac{1}{2\beta(AR)}\right]$ corresponds to the mean-geometric-angle wing.

The same equation with different values for S and (AR) gives the lift on the forward half of the wing, and that on the rear half is obtained by subtraction. For the camber-increment wing, (3) or (6) of figure 4(b), the forward and rear lifts are obtained by using the fact that the tip-cone region of a flat rectangular wing has an average pressure equal to half the two-dimensional value. The details are similar to the method shown in figure 3. The total lift on the forward and rear segments is thus:

	Upwash plus mean flat wing	Camber-increm. wing	Total
For'd β L/q	4.766 A	-3.5 kA	(4.766-3.5k)A
Rear β L/q	3.544 A	+4.5 kA	(3.544+4.5k)A

(B2)

$$\text{Total } \beta \text{ L/q} = (8.31 + k)\, A \qquad \text{(B3)}$$

The lifts acting on the forward and rear segments of the physical wing, multiplied by the respective geometric angles of attack, A(1-k) and A(1+k) give the drag contributions. The total lift and drag are then:

$$L = (8.310 + 1.0k)\, q/\beta\, A \qquad \text{(B4)}$$

$$D = (8.310 - .222\, k + 8.0\, k^2)\, q/\beta\, A^2 \qquad \text{(B5)}$$

Therefore:

$$\ell = \frac{L^2}{DqS} = \frac{(69.056 + 16.620k + 1.0k^2)}{8.310 - .222k + 8.00k^2)\, \beta S} \qquad \text{(B6)}$$

Maximum ℓ occurs where $\frac{d\ell}{dk} = 0$. This leads to the solution:

$$k_{optimum} = .1385 \qquad \text{(B7)}$$

$$\ell_{maximum} = 8.466\, \frac{1}{\beta S} \qquad \text{(B8)}$$

The same procedure can be used to obtain effects of camber alone, upwash alone, or of non-optimum camber.

Results are summarized in Table 1.

Note:

If the wing is mounted at other than zero incidence, equation (B1) may be modified to:

$$\frac{\beta L}{qS} = 4\left(\begin{matrix}\text{Wing angle}\\ \text{of attack}\end{matrix}\right)\left[1 - \frac{1}{2\beta(AR)}\right] \qquad (B9)$$

$$+ 4\left(\begin{matrix}\text{body angle}\\ \text{of attack}\end{matrix}\right)\left(\frac{1}{n-1}\right)\left[1 - \frac{\beta(AR)}{n-1}\left(1-\sqrt{1-\frac{2(n-1)}{n\beta(AR)}}\right)\right]$$

APPENDIX C

METHOD OF ANALYSIS FOR CONTINUOUS CAMBER

Reference 4 describes a method for determining the effect of full-span parabolic camber for a rectangular wing with zero upwash. This method is extended herein to include upwash effects.

From the analysis in reference 4 it may be shown that without upwash but with optimum camber, which is parabolic:

$$\frac{\text{maximum camber}}{\text{chord}} = \frac{A}{8\beta(AR)} \tag{C1}$$

geometric angle of attack of cambered wing as a function of x

$$\alpha_{cam.}(x) = A\left[1 - \frac{1}{2\beta(AR)} + \frac{x}{c}\,\frac{1}{\beta(AR)}\right] \tag{C2}$$

lift coef. due to geometric angle of attack

$$C_{L_{cam.}} = \frac{4A}{\beta}\left[1 - \frac{1}{2\beta(AR)} + \frac{1}{12\beta^2(AR)^2}\right] \tag{C3}$$

drag coef. due to geometric angle of attack

$$C_{D_{cam.}} = \frac{4A^2}{\beta}\left[1 - \frac{1}{2\beta(AR)} + \frac{1}{12\beta^2(AR)^2}\right] \tag{C4}$$

where A is the mean angle of attack of the cambered wing and x is distance along the chord, from the leading edge.

It was shown in Table 1 that the camber that is optimum with upwash does not differ greatly in magnitude or effect from the camber that is optimum without upwash. Accordingly, upwash effect was first determined for the wing cambered as in equation (C1). Slightly more favorable results were then obtained using

the 10 percent greater camber that proved to be optimum with body upwash. The first step is to find the loading on a chord strip, dx, of the upwash wing and multiply this by the local geometric angle of attack of the cambered wing to get the drag contribution. Then wing lift and drag coefficients due to upwash are added to corresponding quantities due to camber, to get values for upwash plus camber.

From equation (B1) of Appendix B the lift of the upwash wing is:

$$L_u = \frac{4A}{\beta} cbq \left[\frac{1}{n-1}\left\{1 - \frac{\beta(AR)}{n-1}\left(1 - \sqrt{1 - \frac{2(n-1)}{n\beta(AR)}}\right)\right\}\right] \qquad (C5)$$

where c is the chord and b the span.

To facilitate a solution for chordwise loading, this equation is expressed in terms of x, representing a variable chord.

Using

$$c = x \qquad b = 2(s-a)$$

$$(AR) = \frac{2(s-a)}{x} = \frac{2a}{x}(n-1) \qquad (C6)$$

gives

$$L_u = \frac{8Aqa}{\beta}\left[x - 2\beta a + 2\beta a \sqrt{1 - \frac{x}{\beta n a}}\right] \qquad (C7)$$

therefore

$$\frac{dL_u}{dx} = \frac{8Aqa}{\beta}\left[1 - \frac{1}{n\sqrt{1 - \frac{x}{\beta n a}}}\right] \qquad (C8)$$

To compute drag, the local geometric angle of attack of the physical wing is used.

$$dD_u = a_{cam.}(x)\, dL_u$$

$$C_{Du} = \frac{1}{qS} \int_{x=0}^{x=c} a_{cam.}(x)\, dL_u \tag{C9}$$

$$= \frac{8A^2 a}{\beta cb} \int_{x=0}^{x=c} \left[1 - \frac{1}{2\beta(AR)} + \frac{x}{c\beta(AR)}\right]\left[1 - \frac{1}{n\sqrt{1-\frac{x}{\beta na}}}\right] dx \tag{C10}$$

For the basic wing-body configuration

$$c = 1$$

$$b = 2$$

$$\beta(AR) = 2$$

$$a = 0.5$$

$$n = 3$$

With these values:

$$\int_{x=0}^{x=c} \left[3/4 + \frac{x}{2}\right]\left[1 - \frac{1}{3\sqrt{1-\frac{x}{1.5}}}\right] dx = .5672 \tag{C11}$$

and

$$C_{Du} = \frac{4}{\beta}(.2836)\, A^2$$

also

$$C_{Lu} = \frac{4}{\beta}(.2887)\, A \text{ from (C5)} \tag{C12}$$

Combining with $C_{L_{cam}}$ and $C_{D_{cam}}$ from (C2) and (C3)

$$C_L = C_{L_{cam.}} + C_{L_u} = \frac{4A}{\beta}(1.059) \tag{C13}$$

$$C_D = C_{D_{cam.}} + C_{D_u} = \frac{4A^2}{\beta}(1.055) \tag{C14}$$

Finally

$$\ell = \frac{C_L^2}{C_D} = 4.252/\beta \tag{C15}$$

For camber without upwash

$$\ell = 3.084/\beta \qquad \text{(C16)}$$

These results are compared with others in Table 2.

REFERENCES

1. Lagerstrom, P. A., and Van Dyke, M. D.: General Considerations About Planar and Nonplanar Lifting Systems. Douglas Aircraft Co., Rept. No. SM-13432, June 1949.

2. Beane, B.: The Effect of Planform on the Lift to Drag Ratio of Wing-Body Combinations at Supersonic Speeds. Douglas Aircraft Co., Rept. No. SM-14454, July 1952.

3. Walker, K.: Examples of Drag Reduction for Rectangular Wings. Douglas Aircraft Co., Rept. No. SM-14446, January 1953.

4. Rott, N.: Minimum Drag Cambered Rectangular Wing for Supersonic Speeds. Jour. Aero. Sci., vol. 20, no. 9, 1953, pp. 642-643.

5. Beskin, L.: Determination of Upwash Around a Body of Revolution at Supersonic Velocities. Consolidated-Vultee Aircraft Corp., Rept. APL/JHU-CM-251, CVAC-DEVF Memo BB-6, May 1946.

6. Graham, E. W.: A Drag Reduction Method for Wings of Fixed Plan Form. Jour. Aero. Sci., vol. 19, no. 12, 1952, pp. 823-825.

7. Coale, C. W.: Supersonic Characteristics of Rectangular Horn-Balanced Ailerons. Douglas Aircraft Co., Rept. No. SM-13718, March 1950.

8. Allen, H. Julian, and Perkins, Edward W.: A Study of Effects of Viscosity on Flow Over Slender Inclined Bodies of Revolution. NACA Rep. 1048, 1951.

9. Sears, W. R. (editor): General Theory of High Speed Aerodynamics. Princeton University Press, 1954.

10. Pitts, William C., Nielsen, Jack N., and Gionfriddo, Maurice P.: Comparison Between Theory and Experiment for Interference Pressure Field Between Wing and Body at Supersonic Speeds. NACA TN 3128, 1954.

11. Tucker, W. A.: Design Considerations for Wings Having Minimum Drag Due to Lift. NACA TN 3317, 1954.

TABLE 1. RESULTS FOR WING OF $\beta(AR) = 2$, TWO-SEGMENT CAMBER, AREA = 2
ZERO INCIDENCE, STANDARD BODY

CONDITION							
Basic Flat Wing	Plus Upwash	Plus Camber	$\beta\ell$	% Gain[1] from Basic	d/β	% Decrease from Basic[2]	Shows Effect of
✓	——	——	3.000	0	.3333	0	——
✓	✓	——	4.155	38.5	.2407	27.8	Upwash
✓	——	k=.125 (optimum)	3.063	2.1	.3265	2.0[3]	Camber
✓	——	k=.138 (not optim.)	3.063	2.1	.3265	2.0	Camber
✓	✓	k=.138 (optimum)	4.233	41.1[4]	.2362	29.1	Upwash + Camber
✓	✓	k=.125 (not optim.)	4.231	41.0	.2364	29.1	Upwash + Camber

Footnotes:

1. Gain in $(C_L)^2$ at a given C_D. Basic case is flat wing, no upwash.
2. Decrease in C_D at a given C_L.
3. This checks result obtained in ref. 3 by different method.
4. Adding camber to upwash case increases ℓ 1.9%; adding upwash to camber case increases ℓ 38.2% .

TABLE 2. EFFECTS OF CONFIGURATION VARIATIONS

CONFIGURATION	% Gain in $\beta\ell$ due to Camber [1]	% Gain in $\beta\ell$ due to Upwash	Supplementary % Gain [2]
Basic, fig. 5(a) $\beta(AR)=2$, $S=2$, $n=3$, 2-segment camber	2.1	38.5	.5
Increased (AR), fig. 5(b) [3] $\beta(AR)=2.5$, $S=2.5$, $n=3.5$	1.3	32.3	.2
Larger body, fig. 5(c) $n=2$	2.1	55.2	.9
3-segment camber, fig. 5(d)	2.5 [4]	38.5	.5
Parabolic camber, fig. 5(e)	2.8	38.5	.7

Footnotes:

[1] Camber used was the optimum for each case.

[2] % gain in $\beta\ell$ is with respect to basic value (3.00) for flat wing, $\beta(AR)=2$, $S=2$, no upwash. Supplementary gain is increment added to sum of separate effects of upwash and camber to give combined effect.

[3] % gain in this row is with respect to value of $\beta\ell$ =3.20 for flat wing with $\beta(AR)=2.5$, $S=2.5$, $n=3.5$.

[4] This figure based on data from ref. 3.

TABLE 3. RESULTS FOR LOW-ASPECT-RATIO TAIL SURFACE IN UNIFORM UPWASH FIELD, $\beta(AR) = 1$, TWO-SEGMENT CAMBER

Upwash angle in °/o mean geom. angle	Optim. camber	°/o gain [1] from basic $\beta\ell$ due to camber alone	°/o gain from basic $\beta\ell$ due to upwash alone	Supplementary °/o gain	°/o decrease from basic d/β due to camber	°/o decrease from basic d/β due to upwash	Supplementary °/o decrease
0	k=.250	12.5	———	———	11.1	———	———
20	k=.272	12.5	20	2.6	11.1	16.7	-1.8 [2]
40	k=.295	12.5 [3]	40	5.6	11.1	28.6	-2.9
———	———	12.5	40	assumed zero	11.1	28.6	-5.3

Footnotes:

[1] Basic $\beta\ell$ for no camber or upwash is 2.0.

[2] Negative value means drag reduction for combined changes is less than sum of separate effects.

[3] 12.5°/o is maximum gain due to camber. For K = .295, camber alone gives smaller gain of 12.1°/o, which would increase supplementary gain to 6°/o.

[4] Comparing -5.3 to -2.9 it is seen that supplementary gain of 5.6°/o in ℓ gave a reduction in d of 2.4°/o.

TABLE 4. EFFECT OF NOSE FORCES ON DRAG AT A GIVEN LIFT. $n = 3$, $2a = 1$, $(AR) = 2$, $S = 2$ TWO-SEGMENT CAMBER, $\beta = 1$, ZERO INCIDENCE

Condition	Lift in terms of wing angle	Wing angle A' for constant lift	Drag for constant lift	% drag reduction from flat wing alone	% drag reduction from preceding value
Flat wing alone	$6\ A'q$	A	$6.000A^2q$	0	——
Flat wing plus upwash [1]	$8.310\ A'q$	$.723\ A$	$4.332A^2q$	27.8	——
Flat wing plus upwash plus nose forces	$9.881\ A'q$ [2]	$.607\ A$	$3.643A^2q$	39.3	15.9
Cambered wing plus upwash [1]	$8.448\ A'q$ [3]	$.711\ A$	$4.252A^2q$	29.1	——
Camber plus upwash plus nose forces	$10.019\ A'q$ [3]	$.598\ A$	$3.588A^2q$ [4]	40.2	15.6

Footnotes:

[1] From Table 1 and Appendix B

[2] A' is wing or body angle. Wing-body lift is $8.310\ A'q$ from Appendix B. Nose lift is $1.571\ A'q$.

[3] Wing lift is $8.448\ A'q$ from Appendix B.

[4] Wing drag is $8.433\ A'^2q$ from Appendix B. Nose drag is $1.571\ A'^2q$.

TABLE 5. MAGNITUDE OF DRAG REDUCTION DUE TO CAMBER FOR PRINCIPAL CONFIGURATIONS. ALL DRAGS ARE FOR LIFT = 6Aq. n = 3, 2a = 1, (AR) = 2, S = 2, TWO-SEGMENT CAMBER, $\beta = 1$

CONDITION			Drag $\times \frac{1}{A^2 q}$	% drag reduction from basic	% drag reduction due to camber[1]
Nose force included	Wing description	Upwash included			
no	flat	no	6.000	0	———
no	optim. camber	no	5.877	2.0	2.0
no	flat zero incidence	yes	4.333	27.8	———
no	opt. camb., zero incid.	yes	4.252	29.1	1.9
yes	flat, zero incid.	yes	3.643	39.3	———
yes	opt. camb., zero incid.	yes	3.588	40.2	1.5
yes	flat, opt. incid.	yes	3.138	47.7	———
yes	opt. camb.,[2] opt. incid.	yes	3.094	48.4	1.4

Footnotes:

[1] % reduction due to camber is with respect to the condition at which camber is applied.

[2] Optimum camber for this case corresponds to k = .18.

TABLE 6. CAMBER EFFECT WITH AND WITHOUT UPWASH

CONDITION			VARIATION IN $\beta\ell$			VARIATION IN d/β		
wing	upwash	camber	no camber	optim. camb.	% increase	no camber	optim. camb.	% decrease
β(AR)=2	none	2-seg.	3.000	3.063	2.1	.3333	.3265	2.0
β(AR)=2	standard body	2-seg.	4.155	4.233	1.9	.2407	.2362	1.9
β(AR)=2	large body	2-seg.	4.657	4.747	1.9	.2147	.2107	1.9
β(AR)=2	none	3-seg.	3.000	3.074	2.5	.3333	.3252	2.4
β(AR)=2	standard body	3-seg.	4.155	4.246	2.2	.2407	.2358	2.0
β(AR)=2	none	parab.	3.000	3.083	2.8	.3333	.3245	2.6
β(AR)=2	standard body	parab.	4.155	4.260	2.5	.2407	.2347	2.5
β(AR)=1	none	2-seg.	2.000	2.250	12.5	.5000	.4444	11.1
β(AR)=1	20%	2-seg.	2.400	2.703	12.6	.4167	.3700	11.2
β(AR)=1	40%	2-seg.	2.800	3.162	12.9	.3571	.3163	11.4

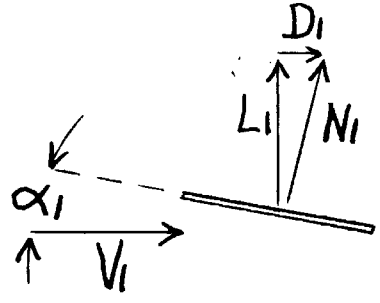

(a) Basic lift and drag.

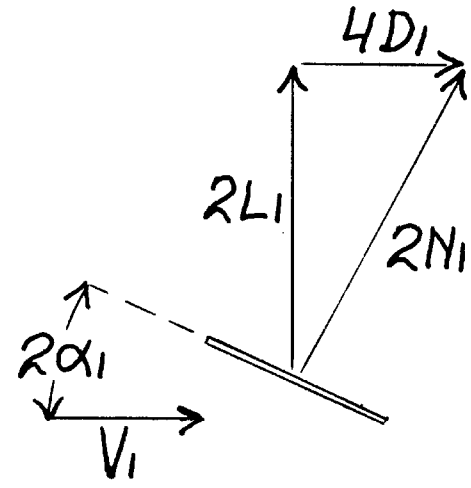

(b) Lift doubled by doubling angle of attack. Drag is quadrupled.

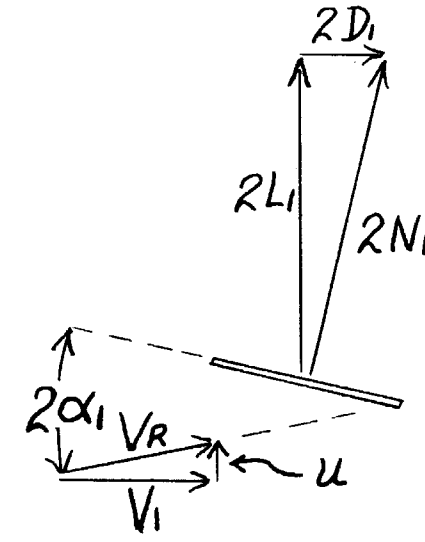

(c) Lift doubled by adding upwash. Drag is doubled.

Figure 1. — How upwash reduces the drag due to lift.

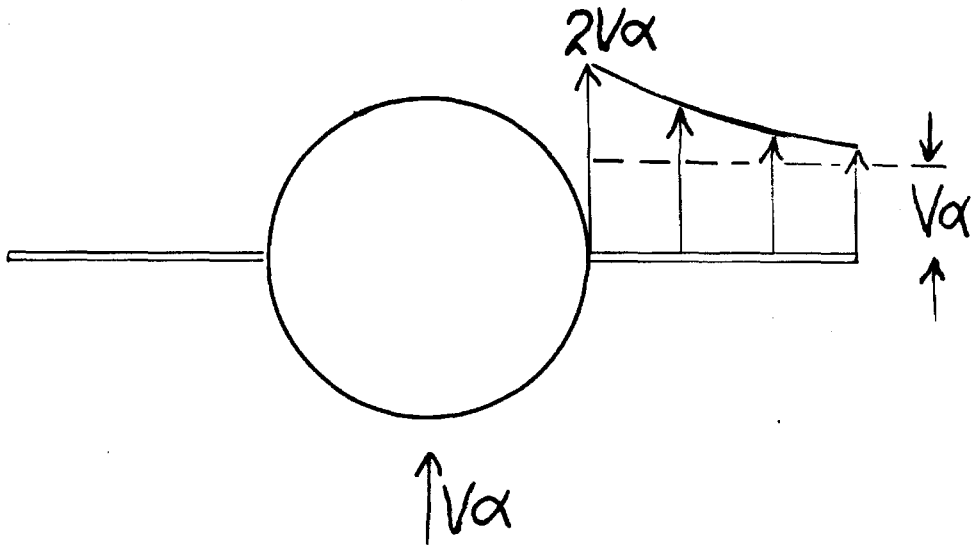

c) Normal-velocity field in wing plane

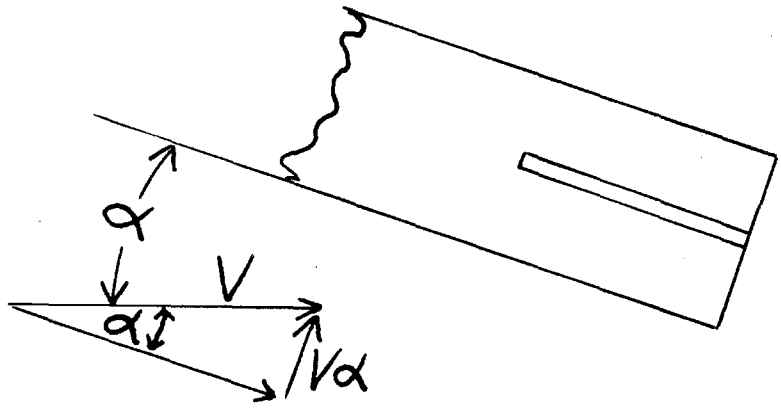

b) Free-stream velocity components

Figure 2. — Wing-body normal-velocity field.

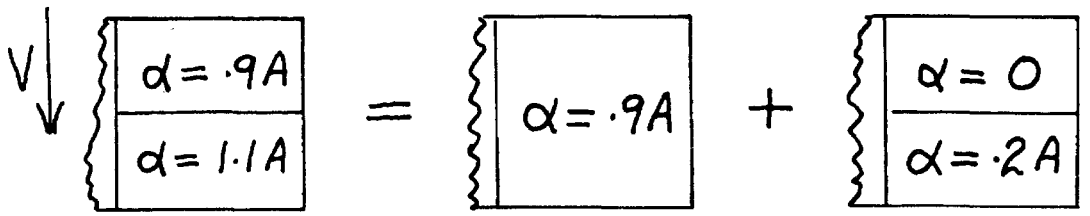

a) Two-segment camber wing as superposition of simpler wings.

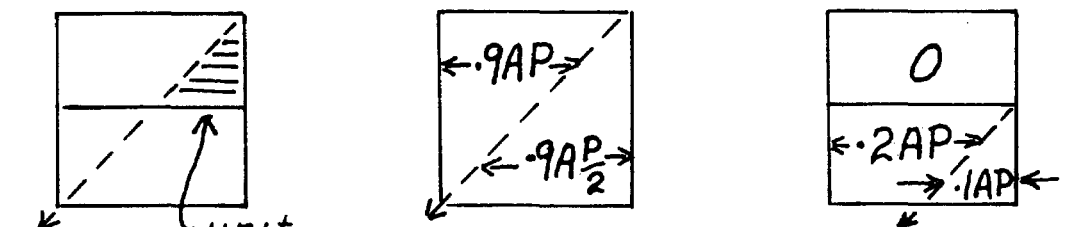

P, 2-dimensional pressure for unit angle of attack.

b) Pressures in various regions.

c) Lift and drag of the cambered wing.

lift on forward half: $3(.9AP) + .9A\frac{P}{2} = 3.15AP$

lift on rear half: $(.9AP) + 3(.9A\frac{P}{2}) + 3(.2AP) + (.1PA) = 2.95AP$

drag: $(3.15AP)(.9A) + (2.95AP)(1.1A) = 6.08A^2P$ (A, radians)

c) To get same lift on uncambered wing

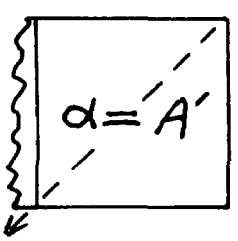

lift = $6A'P$

to get previous lift, $A' = 1.017A$

drag = $6.21\ A^2P$,
an increase of 2.1%

Figure 3.— How camber at the tip reduces drag for a given lift.

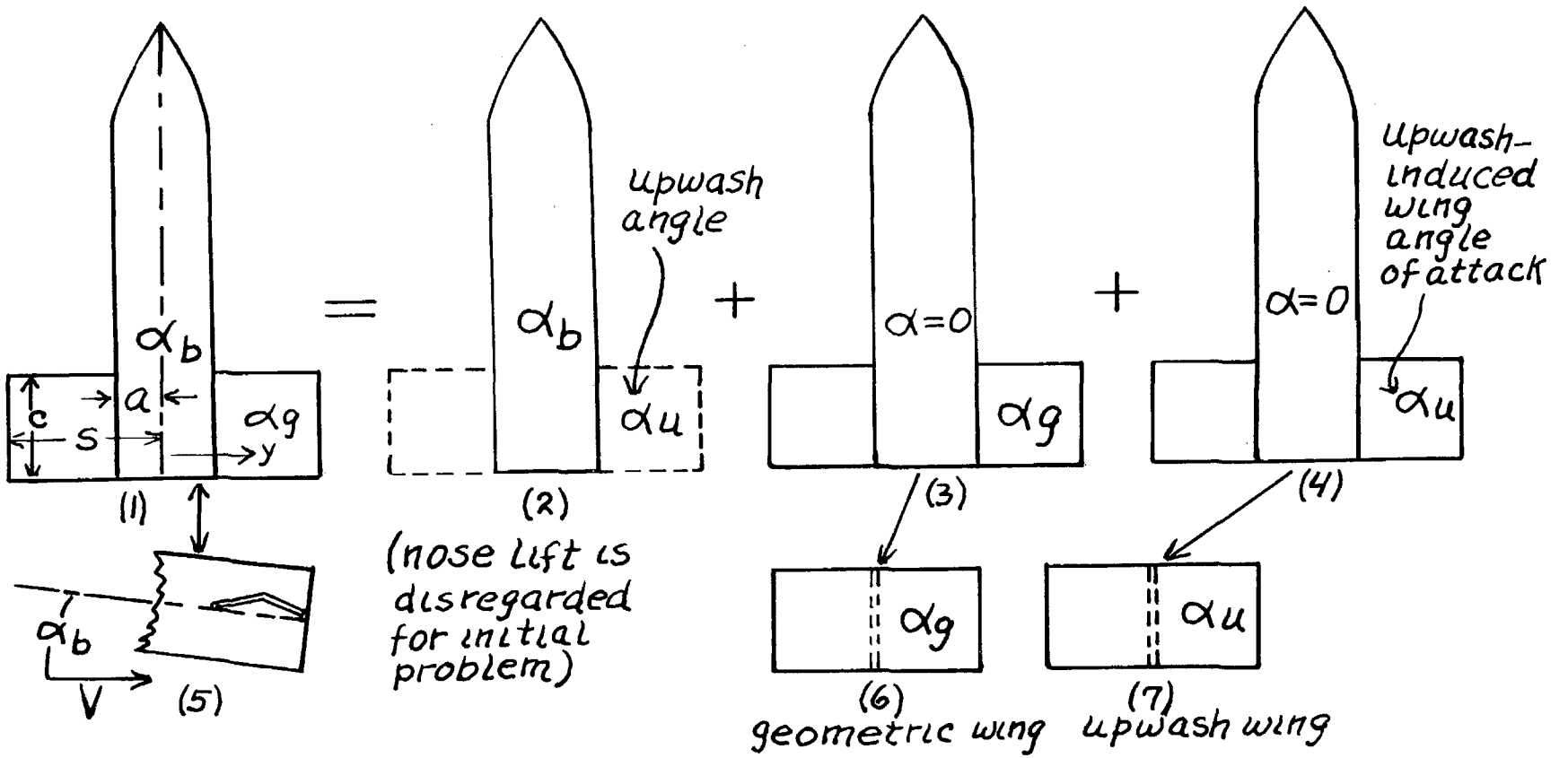

a) Wing-body problem reduced to equivalent exposed-wing problems.

Figure 4.— Superposition procedure for determining wing-body lift.

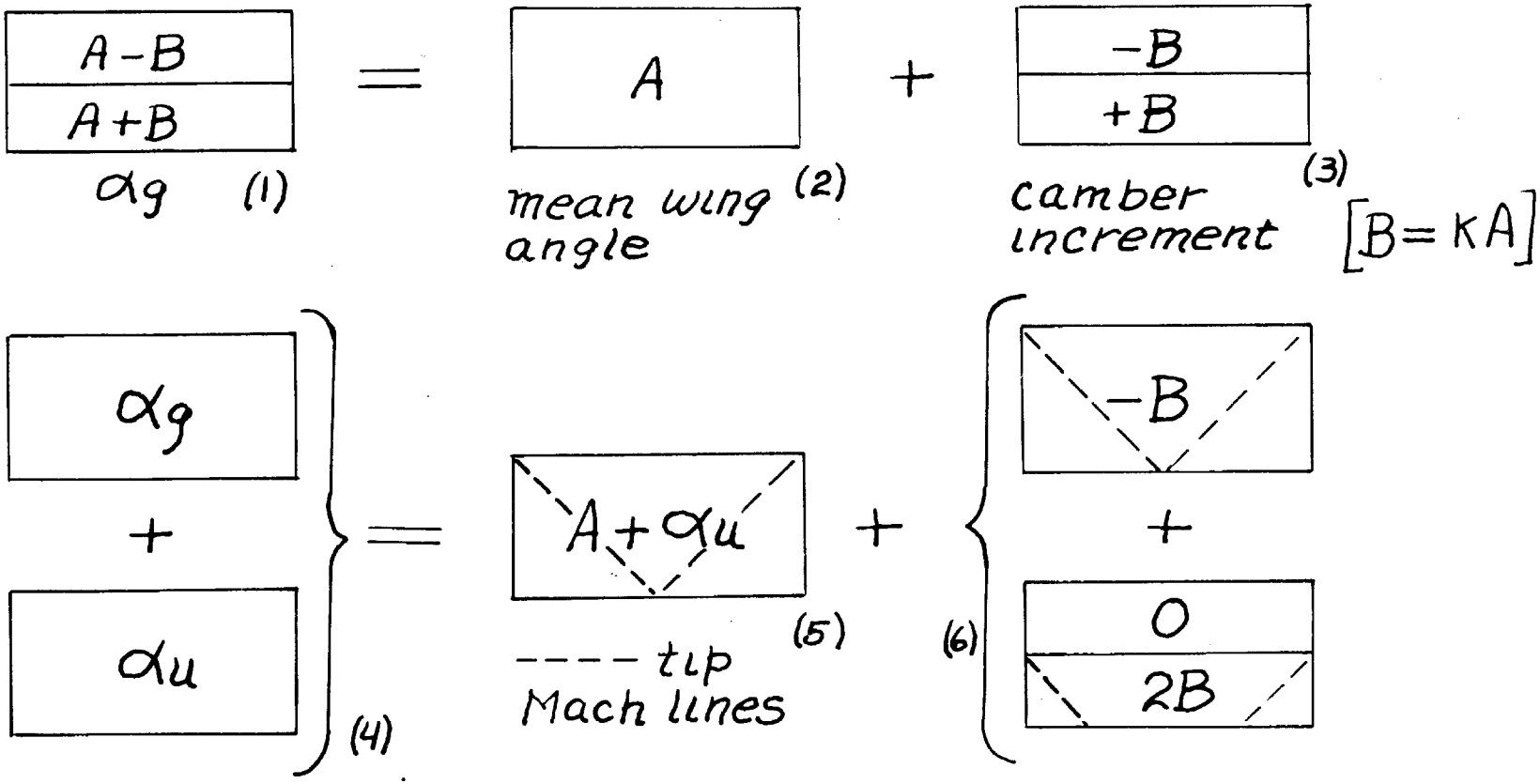

b) Components of the equivalent-wing problem.

Figure 4. — Continued.

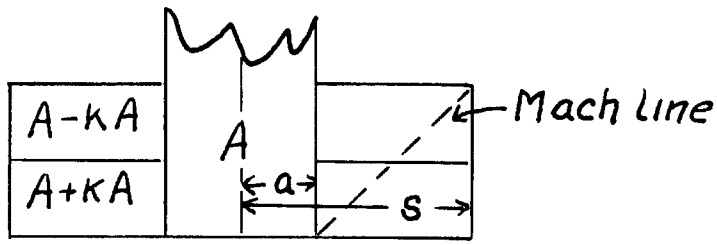

a) Basic configuration, $\beta(AR)=2$, $n=s/a=3$

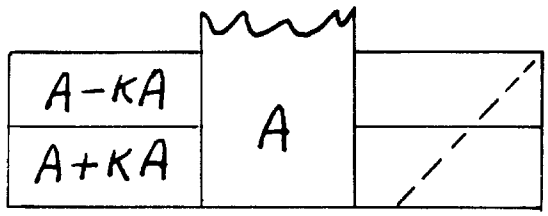

b) Increased aspect ratio, $\beta(AR)=2.5$

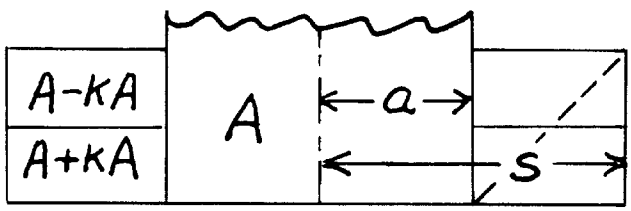

c) Larger body diameter, $s/a=2$

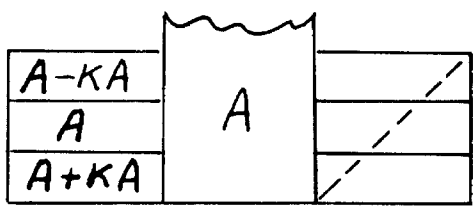

d) Three-segment camber

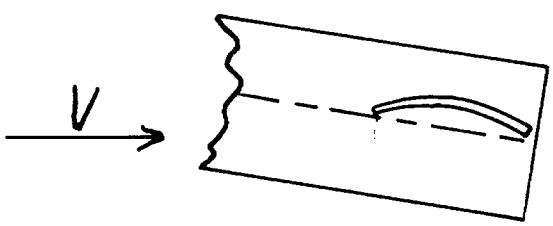

e) Continuous parabolic camber

Figure 5.— Configuration variations.

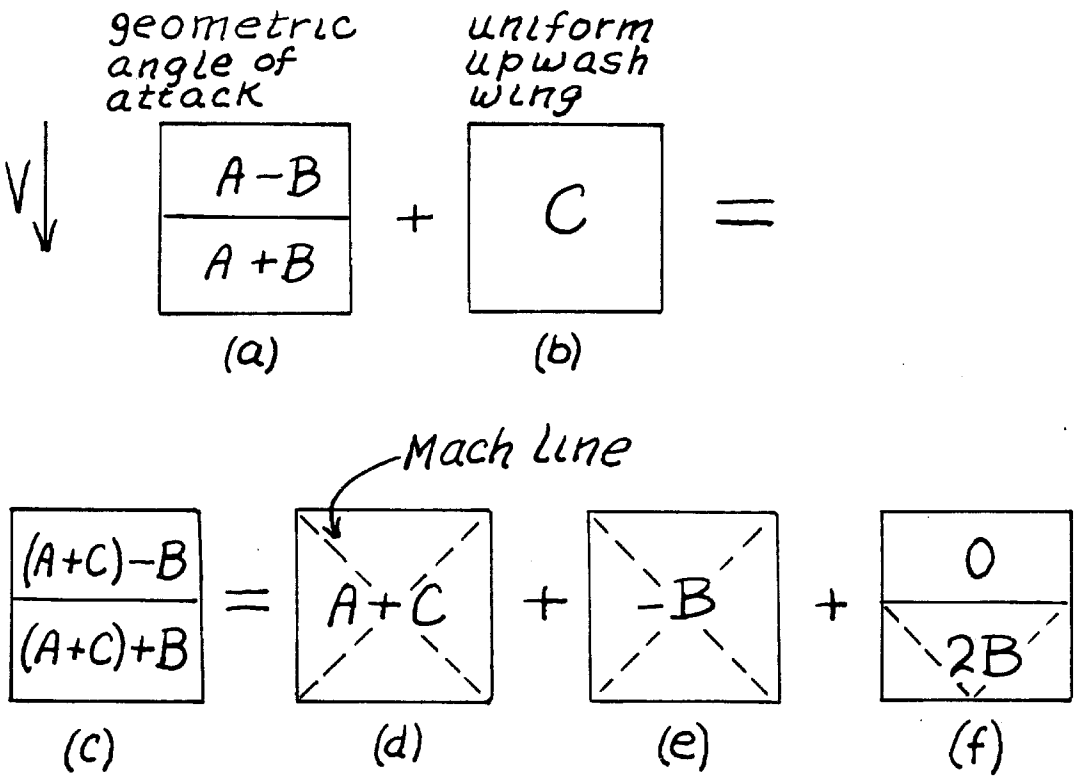

A mean geometric angle

B camber increment angle [$B=KA$].

C uniform upwash angle

Lift for any flat component wing or for wing representing forward half of (d) or (e):

$$C_L = \frac{4\alpha}{\beta}\left[1 - \frac{1}{2\beta(AR)}\right]$$

Figure 6. — Superposition procedure for determining tail lift.

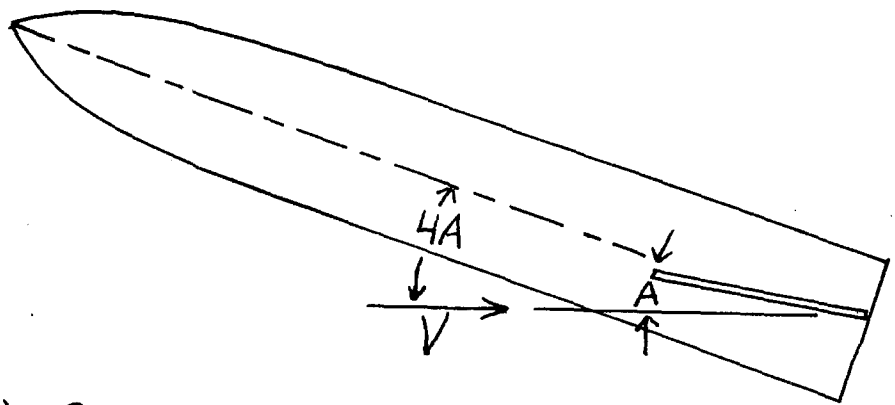

a) Optimum incidence, flat wing

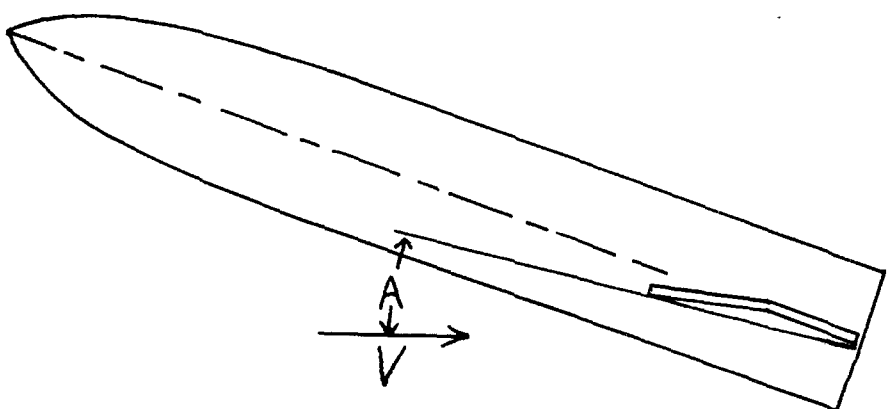

b) Negative-incidence, cambered wing

Figure 7.— Negative-incidence case.

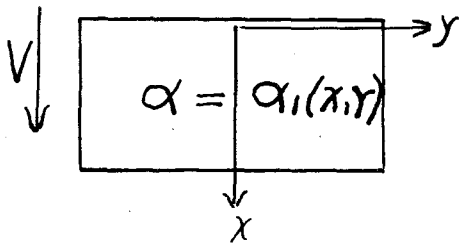

a) arbitrary angle-of-attack distribution

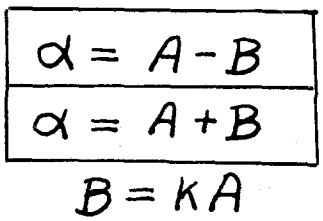

b) example, with two-segment camber

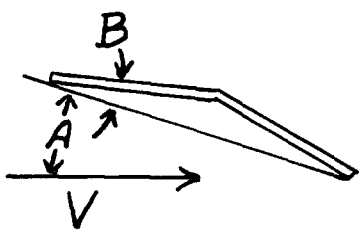

c) two-segment camber $B = kA$, angle of attack of forward part is $(A-B) = A(1-k)$

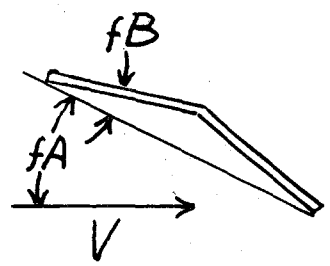

d) all angles increased by factor f, angle of attack of forward part is $f(A-B) = fA(1-k)$

Figure 8.—Wing with local angles of attack maintained proportional to mean angle.